

# Graph Bisection with Pareto-Optimization\*

Michael Hamann, Ben Strasser

Institute of Theoretical Informatics,  
Karlsruhe Institute of Technology,  
P.O. Box 6980, 76128 Karlsruhe, Germany.

michael.hamann@kit.edu, strasser@kit.edu

## Abstract

We introduce FlowCutter, a novel algorithm to compute a set of edge cuts or node separators that optimize cut size and balance in the Pareto-sense. Our core algorithm solves the balanced connected  $st$ -edge-cut problem, where two given nodes  $s$  and  $t$  must be separated by removing edges to obtain two connected parts. Using the core algorithm we build variants that compute node separators and are independent of  $s$  and  $t$ . Using the Pareto-set we can identify cuts with a particularly good trade-off between cut size and balance that can be used to compute contraction and minimum fill-in orders, which can be used in Customizable Contraction Hierarchies (CCH), a speed-up technique for shortest path computations. Our core algorithm runs in  $O(cm)$  time where  $m$  is the number of edges and  $c$  the cut size. This makes it well-suited for large graphs with small cuts, such as road graphs, which are our primary application. For road graphs we present an extensive experimental study demonstrating that FlowCutter outperforms the current state of the art both in terms of cut sizes as well as CCH performance.

---

\*Partial support by DFG grant WA654/19-1 and Google Focused Research Award.

# 1 Introduction

Cutting a graph into two pieces of roughly the same size along a small cut is a fundamental and NP-hard [12] graph problem that has received a lot of attention [2, 7, 15, 17] and has many applications. The application motivating our research is accelerating shortest path computations on roads [3, 6, 9, 13, 20], but in the appendix we also present bisection experiments on non-road graphs. Dijkstra’s algorithm [10] solves the shortest path problem in near-linear time. However, this is not fast enough if the graph consists of a whole continent’s road network. Acceleration algorithms exploit that road networks rarely change and compute auxiliary data in a *preprocessing phase*. This data is independent of the path’s endpoints and can therefore be reused for many shortest path computations. Often the auxiliary data consists of cuts. The basic idea is: Given a graph  $G$  and a cut  $C$  the algorithms precompute for every node how to get to every edge/node in  $C$ . To compute a path the algorithms first determine whether the endpoints are on opposite sides of  $C$  or not. If they are on opposite sides then the algorithms only need to assemble the precomputed paths towards  $C$  and pick the best one. If they are on the same side then the graph search can be pruned at  $C$ . This halves the graph that needs to be searched. As half a continent is still large the idea is applied recursively. The effectiveness of these techniques crucially depends on the size of the cuts found. Fortunately road graphs have small cuts because of geographical features such as rivers or mountains. Previous work has coined the term *natural cuts* for this phenomenon [7]. However, identifying these natural cuts is a difficult problem. Fortunately, as roads change only slowly, preprocessing running times are significantly less important than cut quality. One of these preprocessing-based techniques are *Customizable Contraction Hierarchies* (CCH) [9]. We demonstrate the performance of our algorithms using CCH. The CCH-auxiliary data is tightly coupled with tree-decompositions [4] and minimum fill-in orders. Our algorithms are therefore also applicable in that domain.

Graph partitioning software used for road graphs include *KaHip* [17], *Metis* [15], *Inertial Flow* [19], or *PUNCH* [7]. We experimentally compare FlowCutter with the first three as we unfortunately have no implementation of PUNCH<sup>1</sup>. The cut problem is formalized as a bicriteria problem optimizing the cut size and the imbalance. The *imbalance* measures how much the sizes of both sides differ and is small if the sides are balanced. The standard approach is to bound the imbalance and minimize the cut size. However, this approach has some shortcomings. Consider a graph with a million nodes and set the max imbalance to 1%. An algorithm finds a cut  $C_1$  with 180 edges and 0.9% imbalance. Is this a good cut? It seems good as 180 is small compared to the node count. However, we would come to a different conclusion, if we knew that a cut  $C_2$  with 90 edges and 1.1% imbalance existed. In our application — shortest paths — moving a few nodes to the other side of a cut is no problem. However, halving the cut size has a huge impact. The cut  $C_2$  is thus clearly superior. Further assume that a third cut  $C_3$  with 180 edges and 0.7% existed.  $C_3$  dominates  $C_1$  in both criteria. However, both are equivalent with respect to the standard problem formulation and thus a tool is not required to output  $C_3$  instead of  $C_1$ . To overcome these problems our approach computes a set of cuts that optimize cut size and imbalance in the Pareto sense. A further significant shortcoming of the state-of-the-art partitioners, with the exception of Inertial Flow, is that they were designed for small imbalances. Common benchmarks, such as [21], only include test cases with imbalances up to 5%. However, for our application imbalances of 50% are fine. For such high imbalances unexpected things happen with the standard software, such as increasing the allowed imbalance can increase the achieved cut sizes.

**Contribution.** We introduce FlowCutter, a graph bisection algorithm that optimizes cut size and imbalance in the Pareto sense. The core FlowCutter algorithm solves the balanced edge-*st*-cut graph bisection problem with connected sides. Using this core as subroutine we design

---

<sup>1</sup>Further Microsoft holds a PUNCH-patent which restricts commercial applications.

algorithms to solve the node separator and non-*st* variants. Using these we design a nested dissection-based algorithm to compute contraction node orders as needed by Customizable Contraction Hierarchies (CCH). These orders are also called minimum fill-in orders or elimination orders and can be used to compute good tree-decompositions. We prove that the core algorithm's running time is in  $O(cm)$  where  $m$  is the edge count and  $c$  the cut size. We show in an extensive experimental evaluation that this is a perfect fit for road graphs that are large in terms of edge count but small in terms of cut size.

**Outline.** We define our terminology and introduce related concepts in the preliminaries. The next section introduces the core idea of the *st*-bisection algorithm. In the following section we describe the piercing heuristic, a subroutine needed in the core algorithm. In the section afterwards we describe extensions of the core algorithms: general bisection, node bisection, and computing contraction orders. Finally, we present an experimental evaluation with a comparison against the current state of the art. In the appendix we present further experiments including experiments on non-road graphs, and a detailed running time analysis.

## 2 Preliminaries

A *graph* is denoted by  $G = (V, A)$  with *node set*  $V$  and *arc set*  $A$ . We set  $n := |V|$  and  $m := |A|$ . We consider undirected, simple graphs which we interpret as symmetric directed graphs. Our core algorithm also works on directed graphs which is important for the computation of node separators. A *cut*  $(V_1, V_2)$  is a partition of  $V$  into two disjoint sets  $V_1$  and  $V_2$  such that  $V = V_1 \cup V_2$ . The *size of a cut* is the number of arcs from  $V_1$  to  $V_2$ . A *separator*  $(V_1, V_2, Q)$  is a partition of  $V$  into three disjoint sets  $V_1$ ,  $V_2$  and  $Q$  such that  $V = V_1 \cup V_2 \cup Q$ . No arc connecting  $V_1$  and  $V_2$  must exist. The cardinality of  $Q$  is the *separator's size*. The *imbalance*  $\epsilon \in [0, 1]$  of a cut or separator is defined as the smallest number such that  $\max\{|V_1|, |V_2|\} \leq \lceil (1 + \epsilon)n/2 \rceil$ . An *ST-cut/separator* is a cut/separator between two disjoint node sets  $S$  and  $T$  such that  $S \subseteq V_1$  and  $T \subseteq V_2$ . The *expansion of a cut/separator* is the cut's size divided by  $\min\{|V_1|, |V_2|\}$ . Our method builds upon unit flows that are computed using augmenting paths [11, 1]. A node  $x$  is *source-(target)-reachable* if a non-saturated  $sx$ -path exists with  $s \in S$  ( $t \in T$ ). We denote by  $S_R$  ( $S_T$ ) the set of all *source-(target)-reachable nodes*. The minimum *ST-cut* size corresponds to the maximum *ST-flow* intensity. We define the *source side cut* as  $(S_R, V \setminus S_R)$  and the *target side cut* as  $(T_R, V \setminus T_R)$ . Note that in general max-flows and min-cuts are not unique. However, the source side and target side cuts are.

**Customizable Contraction Hierarchies (CCH)** are an acceleration algorithm for shortest path computations. We only give a high-level overview, as we use CCH only to evaluate the quality of our cuts. No part of FlowCutter builds upon CCH. The details are in [9]. The central operation is the node contraction: Contracting a node  $v$  consists of removing  $v$  and adding edges between all of  $v$ 's unconnected neighbors. The input to CCH consists of a node *contraction order* along which the nodes are iteratively contracted. This yields a supergraph  $G'$  of the input graph. The weights of  $G'$  are computed using an algorithm that essentially enumerates all triangles in  $G'$  in the so-called *customization phase*. Note that contrary to the order computation, having a fast *customization phase* is useful as it allows us to incorporate changes to the weights quickly. Such changes could for example be caused by traffic congestion. CCH can also be used if several weights exist on the same road graph. Having regular cars and trucks is an example of such a situation. The CCH structure can be shared and does not have to be replicated for each weight. It is sufficient to replicate the weights. We therefore discern between memory that is independent of the weights and shared and memory that is needed per weight. Given the weights of  $G'$ , the *shortest path query* consists of a bidirectional search in  $G'$  only following arcs  $(x, y)$  such that  $x$  appears before  $y$  in the order. The search space of a node  $z$  is the subgraph

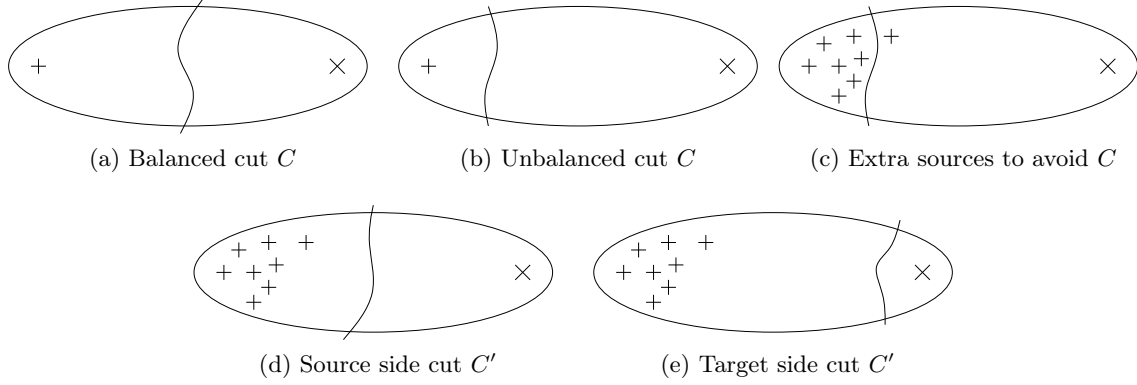


Figure 1: The ellipse represents a graph and the curved lines are cuts. The “+”-signs represent source nodes and “×”-signs represent target nodes.

of  $G'$  that is reachable from  $z$  while only following such arcs. Smaller search spaces yield faster queries. Fewer triangles in  $G'$  yield a faster customization. Less arcs in  $G'$  result in less memory consumption. All these quality metrics depend on the contraction order, whose quality depends on the cuts used in its construction. Finding these cuts is where FlowCutter fits into the big picture.

**Tree-Decompositions.** The constructed supergraph  $G'$  is chordal, which is a graph class tightly coupled with tree-decomposition [4]. The maximum cliques of  $G'$ , which can be efficiently identified in chordal graphs, correspond to the bags of a tree-decomposition. A corresponding tree backbone can be efficiently computed. The maximum clique size in  $G'$  is thus an upper bound to the tree-width of the input graph.

### 3 Core Algorithm

Our algorithm works by computing a sequence of increasingly balanced  $st$ -min-cuts until the imbalance drops below a given input parameter  $\epsilon$ . The intermediate cuts form, after removing dominated ones, the computed Pareto-set. Consider the situation depicted in Figure 1. Initially  $s$  is the only source node and  $t$  is the only target node. We start by computing an  $st$ -min-cut  $C$ , which is the first cut in the sequence. If we are lucky and  $C$  is sufficiently balanced as in Figure 1a our algorithm is finished. However, most of the time we are unlucky and we either have the situation depicted in Figure 1b where the source’s side is too small or the analogous situation where the target’s side is too small. Assume without loss of generality that the source’s side is too small. Our algorithm now transforms non-source nodes into additional source nodes to invalidate  $C$  and computes a new more balanced  $st$ -min-cut  $C'$ , the second cut in the sequence. To invalidate  $C$  our algorithm does two things: It marks all nodes on the source’s side of the cut as source nodes and marks one node as source node on the target’s side that is incident to a cut edge. This node on the target’s side is called the *piercing node* and the corresponding cut arc is called *piercing arc*. The situation is

```

1  $S \leftarrow \{s\}; T \leftarrow \{t\};$ 
2  $S_R \leftarrow S; T_R \leftarrow T;$ 
3 f-grow  $S_R$ ; b-grow  $T_R$ ;
4 while  $S \cap T = \emptyset$  do
5   if  $S_R \cap T_R \neq \emptyset$  then
6     augment flow;
7      $S_R \leftarrow S; T_R \leftarrow T;$ 
8     f-grow  $S$ ; b-grow  $T$ ;
9   else
10    if  $|S_R| \leq |T_R|$  then
11      f-grow  $S$ ;
12      // now  $S = S_R$ 
13      output  $S$ -cut arcs;
14       $x \leftarrow$  pierce node;
15       $S \leftarrow S \cup \{x\};$ 
16       $S_R \leftarrow S_R \cup \{x\};$ 
17      f-grow  $S_R$ ;
18    else
19      // Same for  $T$ 
20      and  $T_R$ 

```

Figure 2:  $st$ -Bisection Algo

illustrated in Figure 1c. All nodes on the source’s side are marked to assure that  $C'$  does not cut through the source’s side. The piercing node is necessary to assure that  $C' \neq C$ . Choosing a good piercing arc is crucial for good quality. In this section we assume that we have a *piercing oracle* that determines the piercing arc given  $C$  in time linear in the size of  $C$ . In Section 4 we describe heuristics to implement such a piercing oracle. We want to achieve that  $C'$  has a better balance than  $C$ . However, this is only true if  $C'$  is a source side cut as in Figure 1d. If  $C'$  is a target side cut as in Figure 1e then  $C'$  might have a worse balance than  $C$ . Luckily, as our algorithm progresses, either the target side will catch up with the balance of the source side or another source side cut is found. In both cases our algorithm eventually finds a cut with a better balance than  $C$ .

Our algorithm computes the *st*-min-cuts by finding max-flows and using the max-flow-min-cut duality [11]. We assign unit capacities to every edge and compute the flow by successively searching for augmenting paths. A core observation of our algorithm is that turning nodes into sources or targets never invalidates the flow. It is only possible that new augmenting paths are created increasing the maximum flow intensity. Given a set of nodes  $X$  we say that *forward growing* (f-grow for short)  $X$  consists of adding all nodes  $y$  to  $X$  for which a node  $x \in X$  and a non-saturated  $xy$ -path exist. Analogously *backward growing*  $X$  (b-grow for short) consists of adding all nodes  $y$  for which a non-saturated  $yx$ -path exists. The growing operations are implemented using a graph traversal algorithm (such as a DFS or BFS) that only follows non-saturated arcs. The algorithm maintains besides the flow values four node sets: the set of sources  $S$ , the set of targets  $T$ , the set source-reachable nodes  $S_R$ , and the set of target-reachable nodes  $T_R$ . Note that an augmenting path exists if and only if  $S_R \cap T_R \neq \emptyset$ . Initially we set  $S = \{s\}$  and  $T = \{t\}$ . Our algorithm works in rounds. In every round it tests whether an augmenting path exists. If one exists the flow is augmented and  $S_R$  and  $T_R$  are recomputed. If no augmenting path exists then it must enlarge either  $S$  or  $T$ . This operation also yields the next cut. It then selects a piercing arc and grows  $S_R$  and  $T_R$  accordingly. The pseudo-code is depicted in Figure 2.

**Running Time Overview.** Assuming a piercing oracle with a running time linear in the current cut size, we can show that the algorithm has a running time in  $O(cm)$  where  $c$  is the size of the most balanced cut found and  $m$  is the number of edges in the graph. The detailed argument requires a non-trivial amortized running time analysis and is in the appendix. However, the core argument is simple: All sets only grow unless we find an augmenting path. As each node can only be added once to each set, the running time between finding two augmenting paths is linear. In total we find  $c$  augmenting paths. The total running time is thus in  $O(cm)$ .

## 4 Pierce Heuristic

In this section we describe how we implement the piercing oracle used in the previous section. Given an unbalanced arc cut  $C$  the piercing oracle should select a piercing arc that is not part of the final balanced cut in at most  $O(|C|)$  time. Piercing the source side and target side cuts and are analogous and we therefore only describe the procedure for the source side. Denote by  $a = (q, p)$  the piercing arc with piercing node  $p \notin S$ .

**Primary Heuristic: Avoid Augmenting Paths.** The first heuristic consists of avoiding augmenting paths whenever possible. Piercing an arc  $a$  leads to an augmenting path if and only if  $p \in T_R$ , i.e., a non-saturated path from  $p$  to a target node exists. As our algorithm has computed  $T_R$  it can determine in constant time whether piercing an arc would increase the size of the next cut. The proposed heuristic consists of preferring edges with  $p \notin T_R$  if possible. It is possible that none or multiple  $p \notin T_R$

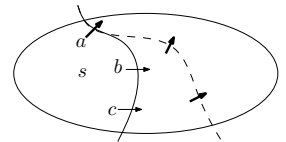


Figure 3: The curves represent cuts, the current one is solid. The arrows are cut-arcs, bold ones result in augmenting paths. The dashed cut is the next cut where piercing any arc results in an augmenting path.

exist. In this case our algorithm employs a further heuristic to choose the piercing arc among them. However, note that the secondary heuristic is often only relevant in the case that none exists. Consider the situation depicted in Figure 3. Suppose for the argument that the target node is still far away and that the perfectly balanced cut is significantly larger. Our algorithm can choose between three piercing arcs  $a$ ,  $b$ , and  $c$ . It will not pick  $a$  as this would increase the cut size. The question that remains is whether  $b$  or  $c$  is better. The answer is that it nearly never matters. Piercing  $b$  or  $c$  does not modify the flow and thus does not change which piercing arcs result in larger cuts. The algorithm will therefore eventually end up with the dashed cut independent of whether  $b$  or  $c$  is pierced. We know that the dashed cut has the same size as all cuts found between the current cut and the dashed cut. Further the dashed cut has the best balance among them and therefore dominates all of them. This means that most of the time our avoid-augmenting-paths heuristic does the right thing. However it is less effective when cuts approach perfect balance. The reason is that the source and target sides meet. When approaching perfect balance our algorithm results in a race between source and target sides to claim the last nodes. Not the best side wins, but the first that gets there.

**Secondary Heuristic: Distance-Based.** Our algorithm picks a piercing arc such that  $\text{dist}(p, t) - \text{dist}(s, p)$  is maximized, where  $s$  and  $t$  are the original source and target nodes. The  $\text{dist}(p, t)$ -term avoids that the source side cut and target side cut meet as nodes close to  $t$  are more likely to be close to the target side cut. Subtracting  $\text{dist}(s, p)$  is motivated by the observation that  $s$  has a high likelihood of being positioned far away from the balanced cuts. A piercing node close to  $s$  is therefore likely on the same side as  $s$ . Our algorithm precomputes the distances from  $s$  and  $t$  to all nodes before the core algorithm is run. This allows it to evaluate  $\text{dist}(p, t) - \text{dist}(s, p)$  in constant time inside the piercing oracle. The distance heuristic has a geometric interpretation as depicted in Figure 4. We interpret the

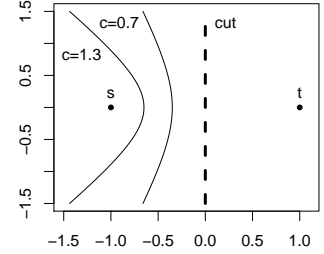


Figure 4: Geometric interpretation of the distance heuristic.

distance as euclidean distance. If  $s$  and  $t$  are points in the plane then the set of points  $p$  for which  $\|p - s\|_2 - \|p - t\|_2 = c$  holds for some constant  $c$  is one branch of a hyperbola. The figure depicts the branches for  $c = 1.3$  and  $c = 0.7$ . The heuristic prefers piecing nodes on the  $c = 1.3$ -branch as it maximizes  $c$ . A consequence of this is that the heuristic works well if the desired cut follows roughly a line perpendicular to the line through  $s$  and  $t$ . This heuristic works on many graphs but there are instances where it breaks down such as cuts that follow a circle-like shape. Note that this geometric interpretation also works in higher-dimensional spaces.

## 5 Extensions

**General Cuts.** Our core algorithm computes balanced  $st$ -cuts. However, in many situations the overall smallest balanced cut is required. This problem variant can be solved with high probability by running FlowCutter multiple times with  $st$ -pairs picked uniformly at random. Indeed, suppose that  $C$  is an optimal cut such that the larger side has  $\alpha n$  nodes (i.e.  $\alpha = (\epsilon + 1)/2$ ) and  $q$  is the number of  $st$ -pairs. The probability that  $C$  separates a random  $st$ -pair is  $2\alpha(1 - \alpha)$ . The success probability over all  $q$   $st$ -pairs is thus  $1 - (1 - 2\alpha(1 - \alpha))^q$ . For  $\epsilon = 33\%$  and  $q = 20$  the success probability is 99.99%. For larger  $\alpha$  this rate decreases. However, it is still large enough for all practical purposes, as for  $\alpha = 0.9$  (i.e.  $\epsilon = 80\%$ ) and  $q = 20$  the rate still is 98.11%. The number of  $st$ -pairs needed does not depend on the size of the graph nor on the cut size. If the instances are run one after another then the running time depends on the worst cut's size which may be more than  $c$ . We therefore run the instances simultaneously and stop once one instance has found a cut of size  $c$ . The running time is thus in  $O(cm)$ .

Note that this argumentation relies on the assumption that it is enough to find an  $st$ -pair

that is separated. However, in practice the positions of  $s$  and  $t$  in their respective sides influences the performance of our piercing heuristic. As a result it is possible that in practice more  $st$ -pairs are needed than predicted by theory.

**Node Separators.** To compute contraction orders node separators are needed and not edge cuts. To achieve this we employ a standard construction to model node capacities in flow problems [1]. We transform the symmetric input graph  $G = (V, A)$  into a directed expanded graph  $G' = (V', A')$  and compute flows on  $G'$ . We expand  $G$  into  $G'$  as follows:

For each node  $x \in V$  there are two nodes  $x_i$  and  $x_o$  in  $V'$ . We refer to  $x_i$  as the *in-node* and to  $x_o$  as the *out-node* of  $x$ . There is an *internal arc*  $(x_i, x_o) \in A'$  for every node  $x \in V$ . We further add for every arc  $(x, y) \in A$  an *external arc*  $(x_o, y_i) \in A'$ . The construction is illustrated in Figure 5. For a source-target pair  $s$  and  $t$  in  $G$  we run the core algorithm with source node  $s_o$  and target node  $t_i$  in  $G'$ . The algorithm computes a sequence of cuts in  $G'$ . Each of the cut arcs in  $G'$  corresponds to a separator node or a cut edge in  $G$  depending on whether the arc in  $G'$  is internal or external. From this mixed cut our algorithm derives a node separator by choosing for every cut edge in  $G$  the endpoint on the larger side. Unfortunately using this construction, it is possible that the graph is separated into more than two components, i.e., we can no longer guarantee that both sides are connected.

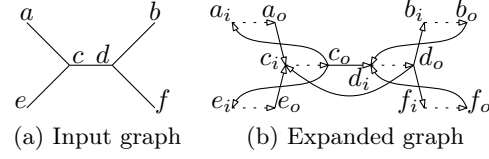


Figure 5: Expansion of an undirected graph  $G$  into a directed graph  $G'$ . The dotted arrows are internal arcs. The solid arrows are external arcs.

**Contraction Orders.** Using a nested dissection [16] variant our algorithm constructs contraction orders. It bisects  $G$  along a node separator  $Q$  into subgraphs  $G_1$  and  $G_2$ . It recursively computes orders for  $G_1$  and  $G_2$ . The order of  $G$  is the order of  $G_1$  followed by the order of  $G_2$  followed by the nodes in  $Q$  in an arbitrary order. Selecting  $Q$  is non-trivial. After some experimentation we went with the following heuristic: Pick the separator with minimum expansion and at most 60% imbalance. As base case for the recursion we use trees and cliques. On cliques any order is optimal and on trees an optimal order can be derived from an optimal node ranking, which can be computed in linear time [18].

Road graphs have many nodes of degree 1 or 2. We exploit this in a fast preprocessing step to significantly reduce the graph size. Our algorithm determines the largest biconnected component  $B$  using [14] in linear time. It then removes all edges from  $G$  that leave  $B$ . It continues independently on every connected component of  $G$ . The resulting orders are concatenated. The order of  $B$  must be last. The other orders can be concatenated in arbitrary way. For each connected component our algorithm identifies the degree-2-chains. For a chain  $x, y_1 \dots y_k, z$  it removes all  $y_i$  and adds an edge from  $x$  to  $z$  unless  $x$  or  $z$  have degree 1. The  $y_i$  nodes and  $x$  or  $z$  if they have degree 1 are positioned at the front of the order. Their relative order is determined using the optimal tree ordering algorithm. All remaining nodes are ordered behind them. After eliminating degree-2-chains our algorithm uses the nested dissection algorithm described above.

## 6 Experiments

We compare Flowcutter to the state-of-the-art partitioners KaHip, Metis, and InertialFlow. We present three experiments: (1) we compare the produced contraction orders in terms of CCH performance, (2) compare the Pareto-cut-sets, and (3) evaluate FlowCutter on non-road graphs using the Walshaw benchmark set. The last experiment is in Appendix A and can be summarized as follows: For  $\epsilon = 5\%$  there are only 6 out of 24 graphs where FlowCutter does not match the best known solutions. For 3 of them FlowCutter is off by at most 5 edges. All experiments were run on a Xeon E5-1630 v3 @ 3.70GHz with 128GB DDR4-2133 RAM.

## 6.1 Order Experiments

We compute contraction orders for 4 DIMACS roads graphs [8]. The smallest is Colorado with  $n = 436K$  and  $m = 1M$ . Next is California and Nevada with  $n = 1.9M$  and  $m = 4.6M$ , followed by (Western) Europe with  $n = 18M$  and  $m = 44M$  and finally a graph encompassing the whole USA with  $n = 24M$  and  $m = 57M$ .

We use FlowCutter with all extensions in two variants denoted by F20 and F3, with 20 respectively 3 random source-target-pairs. We use the `ndmetis` tool of Metis 5.1.0 with the default parameters and refer to it as M. Unfortunately KaHip<sup>2</sup> and InertialFlow do not provide order computation tools. We therefore implemented basic nested dissection ordering algorithms on top of them. The KaHip implementation was already used in [9] and is the current state of the art in terms of order quality. We refer to it as K. The tool iteratively computes cuts using KaHip-strong 0.61 using different random seeds until the cut size does not decrease for 10 rounds. We set  $\epsilon = 20\%$  for KaHip. This value is comparatively small, but KaHip has problems with large  $\epsilon$  as demonstrated in the Pareto-cut experiments in Section 6.2. Note that this setup solely optimizes order quality disregarding order computation times, which therefore can certainly be improved. We report the corresponding running times therefore as upper bounds. Note that we argue that FlowCutter is superior mostly because of the achieved order quality, not because it is particularly fast. Not having well-tuned KaHip running times is therefore not problematic for our comparison. We reimplemented InertialFlow and were able to reproduce the cuts and running times of the original publication with our implementation. It is not randomized and therefore computing several cuts with different random seeds per graph as for KaHip is not useful. As consequence the reported running times adequately represent the performance of a basic nested dissection algorithm combined with Inertial Flow. InertialFlow is denoted by I and we set  $\epsilon = 60\%$ . Both KaHip and InertialFlow compute edge cuts. We turn them into node separators by choosing the endpoints of the cut edges on the larger side.

**Results.** Our results are summarized in Table 1. We observe that, modulo small cache effects, the customization time is correlated with the number of triangles and the average query running time is correlated with the number of arcs in the CCH. The memory needed per weight are correlated with the number of arcs in the CCH. The CCH-structure memory consumption is dominated by the list of precomputed triangles and thus the amount of necessary memory is correlated with the number of triangles. All these correlation are non-surprising and were predicted by CCH theory. Denote by  $n_s$  and  $m_s$  the number of nodes and arcs in the search space. For the average numbers we observe that  $1.7 \leq \frac{n_s(n_s-1)}{2}/m_s \leq 2.6$  and for the maximum numbers we observe that  $2.1 \leq \frac{n_s(n_s-1)}{2}/m_s \leq 3.9$ , which indicates that the search spaces are nearly complete graphs. The number of nodes and the number of arcs are thus related. We can thus say that search space is small or large without indicating whether we refer to nodes or arcs.

FlowCutter produces the smallest search spaces. Using more source-target pairs results in better orders, but already 3 give a decent order. Inertial Flow is dominated by KaHip with the exception of the USA graph. Metis is last by a significant margin on all but the smallest graph. The ratio between the average and the maximum size is very interesting. A high ratio indicates that a partitioner often finds good cuts, but at least one cut is comparatively bad. This ratio is never close to 1, indicating that road graphs are not perfectly homogeneous. In some regions, probably cities, the cuts are worse than in some other regions, probably the countryside. Compared to the competitors, the ratio is however higher for InertialFlow. This illustrates that its geography-based heuristic is effective most of the time but not always.

A small search size is not equivalent with the CCH containing only few arcs. It is possible that vertices are shared between many search spaces and thus the CCH can be significantly smaller than the sum of the search space sizes. This effect occurs and explains why the number

---

<sup>2</sup>Some preliminary work was done in [22].



		Search Space				#Arcs		Up.		Running times				
		Nodes		Arcs [ $\cdot 10^3$ ]		in CCH	#Tri.	Tw.	Bd.	Order	Cust.	Query	Mem. [MiB]	
													per w.	indep.
		Avg.	Max.	Avg.	Max.								[ $\cdot 10^6$ ]	[ $\cdot 10^6$ ]
Col	M	155.6	354	6.1	22	1.4	6.4	102		2.0	18	26	10	61
	K	135.1	357	4.6	22	1.7	7.2	103	$\leq 3$	837.1	21	20	13	70
	I	151.2	542	6.2	38	1.5	7.4	119		7.4	21	25	11	69
	F3	126.3	280	4.1	15	1.3	4.8	91		10.3	15	18	10	48
	F20	122.4	262	3.8	14	1.3	4.4	87		61.0	14	18	10	44
Cal	M	275.5	543	17.3	53	6.5	36.4	180		9.9	88	60	50	335
	K	187.7	483	7.0	37	7.5	34.2	160	$\leq 18$	659.3	90	30	57	326
	I	191.4	605	7.1	53	6.9	34.1	161		42.6	84	31	52	320
	F3	177.5	356	6.2	24	5.9	23.4	127		64.1	69	27	45	231
	F20	170.0	380	5.6	26	5.8	21.8	132		386.8	66	26	44	218
Eur	M	1 223.4	1 983	441.4	933	69.9	1 390.4	926		125.9	2 242	1 162	533	11 210
	K	638.6	1 224	114.3	284	73.9	578.2	482	$\leq 213$	091.1	975	304	564	5 044
	I	732.9	1 569	149.7	414	67.4	589.7	516		1 017.2	932	385	514	5 082
	F3	734.1	1 159	140.2	312	60.3	519.4	531		2 532.7	853	366	460	4 491
	F20	616.0	1 102	102.8	268	58.8	459.6	455		16 841.5	780	271	449	4 024
USA	M	990.9	1 685	249.1	633	86.0	1 241.1	676		170.8	2 084	651	656	10 217
	K	575.5	1 041	71.3	185	97.9	737.1	366	$\leq 265$	567.3	1 250	202	747	6 462
	I	533.6	1 371	62.0	291	88.8	682.0	384		1 076.8	1 122	177	677	5 972
	F3	562.7	906	66.4	159	75.9	478.4	321		2 117.7	856	190	579	4 320
	F20	490.6	868	52.7	154	74.3	440.5	312		12 379.2	811	156	567	4 019

Table 1: Contraction Order Experiments. We report the average and maximum over all nodes  $v$  of the number of nodes and arcs in the CCH-search space of  $v$ , the number of arcs and triangles in the CCH, and the induced upper treewidth bound. We additionally report the order computation times, the customization<sup>3</sup> times, and the average shortest path distance query times. Only the customization times are parallelized using 4 cores. The customization times are the median over 9 runs to eliminate running variance. The query running times are averaged over  $10^6$   $st$ -queries with  $s$  and  $t$  picked uniformly at random. Finally, we report the memory needed per directed 32bit weight, including the input graph weights, and for the weight-independent CCH structure.

of arcs in CCH is orders of magnitude smaller than the sum over the arcs in all search spaces. Further, minimizing the number of arcs in the CCH is not necessarily the same as minimizing the search space sizes. This explains why Metis beats KaHip in terms of CCH size but not in terms of search space size. InertialFlow seems to be comparable to Metis in terms of CCH size, as the CCH arc count is sometimes slightly below and sometimes slightly larger. However, FlowCutter beats all competitors and clearly achieves the smallest CCH sizes.

A third important order quality metric is the number of triangles in the CCH. Metis is competitive on the two smaller graphs, but is clearly dominated on the continental sized graphs. InertialFlow and KaHip seem to be very similar, with the exception of the USA graph where InertialFlow comes out slightly ahead. FlowCutter also wins with respect to this quality metric producing between 20% and 30% less triangles compared to the closest competitor.

As the CCH is essentially a chordal graph which are closely tied to tree decomposition, we obtain upper bounds on the tree width of the input graphs as a side product. This quality metric is not directly related to CCH performance, but is of course indirectly related as most of the other criteria can be bounded in terms of it. As such it reflects the same trend: Metis is worst, followed by InertialFlow, followed by KaHip, and FlowCutter with the best bounds.

<sup>3</sup>Several CCH customization variants exist. Ours is non-amortized, non-perfect, with SSE and uses precomputed triangles. The CCH structure space consumption includes the precomputed triangles.

max $\epsilon$ [%]	Achieved $\epsilon$ [%]				Cut Size				Running Time [s]			
	F20	K	M	I	F20	K	M	I	F20	K	M	I
0	0.000	0.000	0.000	0.000	39	157	51	306	59.8	30.8	0.8	1.1
1	0.169	0.184	0.000	0.566	31	31	52	93	53.2	14.6	0.8	1.4
3	2.293	2.300	0.001	1.112	29	29	61	64	51.0	24.0	0.8	1.7
5	2.293	2.293	0.005	1.571	29	29	42	62	51.0	36.4	0.8	2.3
10	2.293	2.304	0.001	0.642	29	29	43	37	51.0	76.2	0.8	2.2
20	16.706	2.756	0.000	2.656	28	30	41	29	49.6	15.0	0.9	2.4
30	16.706	2.768	13.936	5.484	28	29	51	29	49.6	15.5	0.8	2.9
50	49.058	2.768	0.000	40.833	24	29	39	27	43.2	15.5	0.8	3.7
70	49.058	2.768	41.178	42.591	24	29	4310	26	43.2	15.4	0.8	4.9
90	89.838	2.768	47.370	85.555	14	29	3711	18	25.4	15.6	0.9	5.2

(a) California and Nevada

max $\epsilon$ [%]	Achieved $\epsilon$ [%]				Cut Size				Running Time [s]			
	F20	K	M	I	F20	K	M	I	F20	K	M	I
0	0.000	0.000	0.000	0.000	240	716	369	1180	1390.3	369.1	3.3	4.3
1	0.132	0.998	0.000	0.089	220	245	360	391	1342.9	80.2	3.3	7.9
3	0.132	0.457	0.000	0.008	220	227	372	319	1342.9	112.5	3.1	10.2
5	4.894	0.464	0.000	0.857	213	227	369	276	1319.0	158.3	3.3	12.3
10	9.330	0.043	0.000	0.375	180	228	375	241	1181.5	338.1	3.1	16.8
20	10.542	3.139	0.000	0.132	162	250	375	220	1089.5	75.5	3.1	25.6
30	10.542	3.139	0.017	7.384	162	250	369	203	1089.5	75.4	3.1	34.9
50	44.386	3.139	33.336	10.542	155	250	9881	162	1047.8	75.3	3.2	47.5
70	66.655	3.139	41.178	44.386	86	250	14375	155	591.6	75.5	3.2	82.8
90	84.199	3.139	83.087	84.257	13	250	28	17	92.8	75.4	3.3	17.1

(b) Central Europe

Table 2: Pareto-Set Experiments. We report the balance, the cut size and the computation time for various partitioners and allowed maximum imbalance. For FlowCutter the computation time includes the time needed to compute all less balanced cuts in the Pareto cut set.

Quality comes at a price and thus the computation times of the orders follow the opposite trend: FlowCutter is the slowest, followed by InertialFlow, while Metis is astonishingly fast. Where KaHip fits into the picture is unclear, as the nested dissection implementation employed is not tuned for computation speed and only for order quality. However, the times in the next experiment suggested that a well-tuned implementation is between FlowCutter and InertialFlow.

## 6.2 Pareto Cut Set Experiments

In the previous experiment we have demonstrated that FlowCutter produces the best contraction orders. In this section we look at the Pareto-cut sets of two graph in more detail. Selecting meaningful and representative testing instances is difficult. The cuts of the USA graph are dominated by the cut induced by the Mississippi, as is demonstrated in Appendix C. The Europe graph is problematic as the top level cuts behave differently from nearly all lower level cuts. On the top level there are many comparatively weakly connected peninsulas. This structure is very rare on the lower levels. This leads to a special behavior that we discuss in detail in Appendix B which can be summarized as following: Cutting the peninsulas leads to a smaller cut but only delays the inevitable cut through central Europe in a recursive setup. Cutting the peninsulas thus looks clearly better, even though it is not clearly superior when considering a recursive partitioning. We therefore run experiments on a subgraph of the Europe with a latitude  $\in [45, 52]$

and longitude  $\in [-2, 11]$  that encompasses most of Central Europe, i.e., with all the peninsulas cut off. We additionally pick the DIMACS California&Nevada graph because [5] determined an optimal cut of this graph for  $\epsilon = 0$ . The Appendix C additionally contains numbers for the Colorado graph. We compare KaHip 0.71, Metis 5.1.0, InertialFlow and FlowCutter-20 in terms of edge cut sizes. The first three compute a single cut, whereas FlowCutter computes a Pareto-set, such as the one illustrated in Figure 6. We therefore run the first three for various choices of  $\epsilon$ . We use KaHip-strong with `--enforce_balance` for  $\epsilon = 0$ . All other parameters have default values.

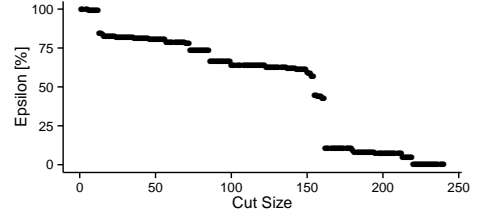


Figure 6: F20 Pareto cuts, C. Europe.

**Results.** Table 2 summarizes our results. Metis produces extremely bad cuts for imbalances above 70%. Strangely KaHip has problems with perfect balance. This is unexpected as KaHip was optimized for perfect balance [17]. This is most likely the result of the default parameters not being optimized for road graphs. KaHip and Metis mostly ignore the allowed imbalance. The maximum achieved imbalance of KaHip is 3.2% even though 90% is allowed. Metis is nearly always well below 1%. Interestingly increasing the allowed imbalance can increase the achieved cut sizes. We conclude that computing a full Pareto-cut-set for a road graph is not possible in the straight-forward way with KaHip or Metis.

InertialFlow is bad at finding highly balanced cuts. Fortunately, for higher values of  $\epsilon$  competitive cuts are found. This explains why the computed contraction orders are competitive. A significant advantage of InertialFlow compared to Metis and KaHip is that a higher maximum imbalance cannot increase the cut size. Unfortunately, InertialFlow has its own set of problems. It does not find the best cut just below the allowed maximum imbalance. For example the good cut through Europe with  $\epsilon = 10.542\%$  is not found when allowing a maximum imbalance of 30%. A maximum imbalance of 50% is necessary, i.e., the choice of 30% vs 50% determines whether a 10.5% cut is found or not. Unfortunately, a higher maximum imbalance is not always better. Consider the two cuts with 29 edges on California. They differ in the achieved balance, i.e., two cuts with the same size but a different balance exist. InertialFlow does not find the variant with the better balance, if the maximum allowed imbalance is too high. Further, it fails to find the 29 edge cut with the best balance which is only found by KaHip and FlowCutter. Unfortunately, also KaHip can not find it reliably, as it finds 4 different cuts with 29 edges and varying balances. Only FlowCutter reliably finds the variant with the best balance. In [5] an optimal California cut for  $\epsilon = 0\%$  with 32 edges was computed. All tested algorithms are therefore suboptimal as the best one finds a cut with 39 edges. However, even a slight imbalance of 1% is enough for FlowCutter and KaHip to find cuts with 31 edges. The achieved 1% cuts can therefore be optimal. Metis is the fastest, followed by InertialFlow, followed by KaHip. Positioning FlowCutter in this list is difficult, as it (a) is the only one to compute Pareto cut set, enabling plots such as those in Figure 6, and (b) even if one is only interested in a single cut, it honors the maximum imbalance parameter much better.

## 7 Conclusion and Future Research

We introduced FlowCutter, a bisection algorithm that optimizes balance and cut size in the Pareto sense. We used it to compute contraction orders (also called elimination or minimum fill-in orders) and have shown that it beats the state of the art in terms of quality on road graphs.

FlowCutter needs two initial nodes on separate sides of the cut. Currently these are determined by random sampling. A better selection strategy could decrease the number of samples needed. Further investigating other piercing heuristics could be beneficial.

**Acknowledgment:** We thank Roland Glantz for helpful discussions.

## References

- [1] Ravindra K. Ahuja, Thomas L. Magnanti, and James B. Orlin. *Network Flows: Theory, Algorithms, and Applications*. Prentice Hall, 1993.
- [2] David A. Bader, Henning Meyerhenke, Peter Sanders, and Dorothea Wagner. *Graph Partitioning and Graph Clustering: 10th DIMACS Implementation Challenge*, volume 588. American Mathematical Society, 2013.
- [3] Hannah Bast, Daniel Delling, Andrew V. Goldberg, Matthias Müller–Hannemann, Thomas Pajor, Peter Sanders, Dorothea Wagner, and Renato F. Werneck. Route planning in transportation networks. Technical Report abs/1504.05140, ArXiv e-prints, 2015.
- [4] Hans L. Bodlaender. Treewidth: Structure and algorithms. In *Proceedings of the 14th International Colloquium on Structural Information and Communication Complexity*, Lecture Notes in Computer Science. Springer, 2007.
- [5] Daniel Delling, Daniel Fleischer, Andrew V. Goldberg, Ilya Razenshteyn, and Renato F. Werneck. An exact combinatorial algorithm for minimum graph bisection. *Mathematical Programming*, pages 1–24, 2014.
- [6] Daniel Delling, Andrew V. Goldberg, Thomas Pajor, and Renato F. Werneck. Customizable route planning in road networks. *Transportation Science*, 2014. accepted for publication.
- [7] Daniel Delling, Andrew V. Goldberg, Ilya Razenshteyn, and Renato F. Werneck. Graph partitioning with natural cuts. In *25th International Parallel and Distributed Processing Symposium (IPDPS’11)*, pages 1135–1146. IEEE Computer Society, 2011.
- [8] Camil Demetrescu, Andrew V. Goldberg, and David S. Johnson, editors. *The Shortest Path Problem: Ninth DIMACS Implementation Challenge*, volume 74 of *DIMACS Book*. American Mathematical Society, 2009.
- [9] Julian Dibbelt, Ben Strasser, and Dorothea Wagner. Customizable contraction hierarchies. In *Proceedings of the 13th International Symposium on Experimental Algorithms (SEA’14)*, volume 8504 of *Lecture Notes in Computer Science*, pages 271–282. Springer, 2014.
- [10] Edsger W. Dijkstra. A note on two problems in connexion with graphs. *Numerische Mathematik*, 1:269–271, 1959.
- [11] Lester R. Ford, Jr. and Delbert R. Fulkerson. Maximal flow through a network. *Canadian Journal of Mathematics*, 8:399–404, 1956.
- [12] Michael R. Garey and David S. Johnson. *Computers and Intractability. A Guide to the Theory of  $\mathcal{NP}$ -Completeness*. W. H. Freeman and Company, 1979.
- [13] Martin Holzer, Frank Schulz, and Dorothea Wagner. Engineering multilevel overlay graphs for shortest-path queries. *ACM Journal of Experimental Algorithmics*, 13(2.5):1–26, December 2008.
- [14] John E. Hopcroft and Robert E. Tarjan. Efficient algorithms for graph manipulation. *Communications of the ACM*, 16(6):372–378, June 1973.
- [15] George Karypis and Vipin Kumar. A fast and high quality multilevel scheme for partitioning irregular graphs. *SIAM Journal on Scientific Computing*, 20(1):359–392, 1999.
- [16] Richard J. Lipton, Donald J. Rose, and Robert Tarjan. Generalized nested dissection. *SIAM Journal on Numerical Analysis*, 16(2):346–358, April 1979.

- [17] Peter Sanders and Christian Schulz. Think locally, act globally: Highly balanced graph partitioning. In *Proceedings of the 12th International Symposium on Experimental Algorithms (SEA'13)*, volume 7933 of *Lecture Notes in Computer Science*, pages 164–175. Springer, 2013.
- [18] Alejandro A. Schæffer. Optimal node ranking of trees in linear time. *Information Processing Letters*, 33:91–96, November 1989.
- [19] Aaron Schild and Christian Sommer. On balanced separators in road networks. In *Proceedings of the 14th International Symposium on Experimental Algorithms (SEA'15)*, Lecture Notes in Computer Science. Springer, 2015.
- [20] Frank Schulz, Dorothea Wagner, and Karsten Weihe. Dijkstra’s algorithm on-line: An empirical case study from public railroad transport. *ACM Journal of Experimental Algorithmics*, 5(12):1–23, 2000.
- [21] A. J. Soper, Chris Walshaw, and Mark Cross. A combined evolutionary search and multilevel optimisation approach to graph partitioning. *Journal of Global Optimization*, 29(2):225–241, 2004.
- [22] Michael Wegner. Finding small node separators. Bachelor thesis, Karlsruhe Institute of Technology, October 2014.

## A Walshaw Benchmark Set

A popular set of graph partitioning benchmark instances is maintained by Walshaw [21]. The data contains 34 graphs and solutions to the edge-bisection problem with non-connected sides and maximum imbalance values of  $\epsilon = 0\%$ ,  $\epsilon = 1\%$ ,  $\epsilon = 3\%$ , and  $\epsilon = 5\%$ . These archived solutions are the best cuts that any partitioner has found so far. A few of them were even proven to be optimal [5]. Comparing against these archived solutions allows us to compare FlowCutter quality-wise against the state of the art. We want to stress that this state of the art was computed by a large mixture of algorithms with an even larger set of parameters that may have been chosen in instance-dependent ways. We compare this against a single algorithm with a single set of parameters. Further FlowCutter was designed for higher imbalances than 5%. It was not tuned for the cases with a lower imbalance. FlowCutter only computes cuts with connected sides. We therefore filter out all graphs that are either not connected or where the archived  $\epsilon = 0$ -solution has non-connected sides. Of the 34 graphs only 24 remain. The results are reported in Tables 3 and 4.

For  $\epsilon = 5\%$  there are only 6 graphs where FlowCutter does not match the best known cut quality. These are: “144”, “cs4”, “m14b”, “wave”, “wing”, and “wing\_nodal”. For three of these graphs FlowCutter finds cuts that are larger by a negligible amount of at most 5 edges. For the other three the cuts found are larger but are still close to the best known solutions. For lower imbalances the results are not quite as good but still very close to the best known solutions.

In terms of running time the results are more mixed. Some cuts are found very quickly, while FlowCutter needs a significant amount of time on others. This is due to the fact that its running time is in  $O(cm)$ . If both the cut size  $c$  and the edge count  $m$  are large then this running time is high. However, for graphs with small cuts the algorithm scales nearly linearly in the graph size. Note that FlowCutter does not only compute the highly balanced cuts reported in the table.

graph	algorithm	minimum edges in cut for				running time [s]
		$\epsilon = 0\%$	$\epsilon = 1\%$	$\epsilon = 3\%$	$\epsilon = 5\%$	
144	FlowCutter 20	6 649	6 608	6 514	6 472	2 423.82
144K nodes	FlowCutter 100	6 515	6 479	6 456	6 366	10 437.91
1074K edges	Reference	6 486	6 478	6 432	6 345	
3elt	FlowCutter 20	90	89	87	87	0.36
4720 nodes	FlowCutter 100	90	89	87	87	1.87
13K edges	Reference	90	89	87	87	
4elt	FlowCutter 20	149	138	137	137	1.97
15K nodes	FlowCutter 100	139	138	137	137	9.50
45K edges	Reference	139	138	137	137	
598a	FlowCutter 20	2 417	2 390	2 367	2 336	545.69
110K nodes	FlowCutter 100	2 400	2 388	2 367	2 336	2 675.32
741K edges	Reference	2 398	2 388	2 367	2 336	
auto	FlowCutter 20	10 609	10 283	9 890	9 450	13 445.66
448K nodes	FlowCutter 100	10 549	10 283	9 823	9 450	66 249.82
3314K edges	Reference	10 103	9 949	9 673	9 450	
bcsstk30	FlowCutter 20	6 454	6 347	6 251	6 251	245.65
28K nodes	FlowCutter 100	6 408	6 347	6 251	6 251	1 230.27
1007K edges	Reference	6 394	6 335	6 251	6 251	
bcsstk33	FlowCutter 20	10 220	10 097	10 064	9 914	118.38
8738 nodes	FlowCutter 100	10 177	10 097	10 064	9 914	573.02
291K edges	Reference	10 171	10 097	10 064	9 914	
brack2	FlowCutter 20	742	708	684	660	58.13
62K nodes	FlowCutter 100	742	708	684	660	283.99
366K edges	Reference	731	708	684	660	
crack	FlowCutter 20	184	183	182	182	2.17
10K nodes	FlowCutter 100	184	183	182	182	10.97
30K edges	Reference	184	183	182	182	
cs4	FlowCutter 20	381	371	367	360	11.68
22K nodes	FlowCutter 100	372	370	365	357	58.11
43K edges	Reference	369	366	360	353	
cti	FlowCutter 20	342	318	318	318	6.10
16K nodes	FlowCutter 100	339	318	318	318	30.55
48K edges	Reference	334	318	318	318	
fe_4elt2	FlowCutter 20	130	130	130	130	1.86
11K nodes	FlowCutter 100	130	130	130	130	9.19
32K edges	Reference	130	130	130	130	

Table 3: Performance on the Walshaw benchmark set, Part 1. “Reference” is the best known bisection for the graph as maintained by Walshaw. “FlowCutter 20” uses 20 random *st*-pairs and “FlowCutter 100” uses 100 random *st*-pairs.

graph	algorithm	minimum edges in cut for				running time [s]
		$\epsilon = 0\%$	$\epsilon = 1\%$	$\epsilon = 3\%$	$\epsilon = 5\%$	
fe_ocean	FlowCutter 20	504	431	311	311	89.70
143K nodes	FlowCutter 100	483	408	311	311	418.60
409K edges	Reference	464	387	311	311	
fe_rotor	FlowCutter 20	2 115	2 091	1 959	1 948	334.58
99K nodes	FlowCutter 100	2 106	2 067	1 959	1 940	1 636.78
662K edges	Reference	2 098	2 031	1 959	1 940	
fe_sphere	FlowCutter 20	386	386	384	384	5.98
16K nodes	FlowCutter 100	386	386	384	384	30.84
49K edges	Reference	386	386	384	384	
fe_tooth	FlowCutter 20	3 852	3 841	3 814	3 773	413.48
78K nodes	FlowCutter 100	3 836	3 832	3 790	3 773	2 067.54
452K edges	Reference	3 816	3 814	3 788	3 773	
finan512	FlowCutter 20	162	162	162	162	8.11
74K nodes	FlowCutter 100	162	162	162	162	39.01
261K edges	Reference	162	162	162	162	
m14b	FlowCutter 20	3 858	3 826	3 823	3 805	2 115.07
214K nodes	FlowCutter 100	3 836	3 826	3 823	3 804	10 512.24
1679K edges	Reference	3 836	3 826	3 823	3 802	
t60k	FlowCutter 20	80	79	73	65	2.98
60K nodes	FlowCutter 100	80	77	71	65	14.55
89K edges	Reference	79	75	71	65	
vibrobox	FlowCutter 20	10 614	10 356	10 356	10 356	139.90
12K nodes	FlowCutter 100	10 365	10 310	10 310	10 310	680.76
165K edges	Reference	10 343	10 310	10 310	10 310	
wave	FlowCutter 20	8 734	8 734	8 734	8 724	2 723.12
156K nodes	FlowCutter 100	8 716	8 673	8 650	8 590	13 583.59
1059K edges	Reference	8 677	8 657	8 591	8 524	
whitaker3	FlowCutter 20	127	126	126	126	1.49
9800 nodes	FlowCutter 100	127	126	126	126	7.00
28K edges	Reference	127	126	126	126	
wing	FlowCutter 20	790	790	790	790	80.11
62K nodes	FlowCutter 100	790	790	781	773	401.82
121K edges	Reference	789	784	773	770	
wing_nodal	FlowCutter 20	1 767	1 764	1 715	1 691	27.02
10K nodes	FlowCutter 100	1 743	1 740	1 710	1 688	134.05
75K edges	Reference	1 707	1 695	1 678	1 668	

Table 4: Performance on the Walshaw benchmark set, Part 2.



max $\epsilon$ [%]	Achieved $\epsilon$ [%]				Cut Size				Running Time [s]			
	F20	K	M	I	F20	K	M	I	F20	K	M	I
0	0.000	0.000	0.003	0.000	276	1 296	402	1 579	3 475.5	1 887.5	8.9	11.3
1	0.930	1.000	0.003	0.337	234	169	398	417	3 292.7	224.7	8.9	19.0
3	2.244	2.717	0.003	0.357	221	130	306	340	3 215.0	317.5	8.9	28.0
5	4.918	2.976	0.003	0.171	216	129	276	299	3 181.7	510.2	8.9	33.6
10	9.453	8.092	0.003	0.174	188	112	460	284	2 913.3	934.0	9.0	49.3
20	9.453	9.405	0.003	7.539	188	126	483	229	2 913.3	198.8	8.9	69.9
30	9.453	9.232	0.003	9.060	188	128	465	202	2 913.3	193.6	8.9	94.0
50	42.080	9.232	33.336	9.453	58	128	31 127	188	949.4	194.1	9.1	172.9
70	67.497	9.232	41.178	64.724	22	128	53 365	38	371.9	193.9	9.4	79.0
90	72.753	9.232	70.741	72.753	2	128	44	2	51.9	194.1	9.0	18.9

Table 5: Results for the DIMACS Europe graph with 18M nodes and 22M edges. The KaHip cut with 169 edges does not have connected sides.

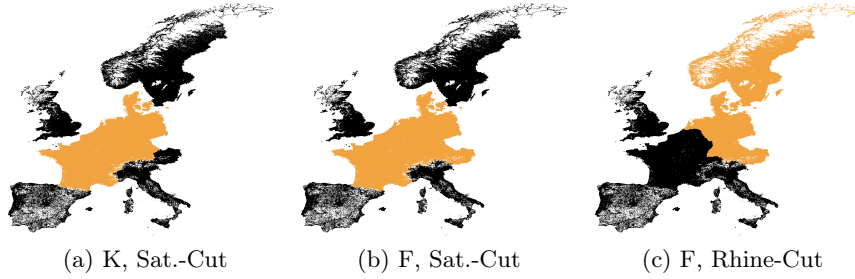


Figure 7: Various good cuts found. "K" is a cut found with KaHip. "F" was found with FlowCutter.

## B Europe Graph

We performed bisection experiments on the DIMACS Europe graph. The results are presented in Table 5. The KaHip 112-edge cut is illustrated in Figure 7a and the 188-edge cut of FlowCutter is depicted in Figure 7c. The reason is that our piercing heuristic searches for cuts that are roughly perpendicular to a line whereas the cut found by KaHip is roughly a circle. This is due to Europe's very special topology. It consists of a well connected center consisting of France, Germany, Belgium, Luxembourg, the Netherlands and Denmark. This center is surrounded by 4 satellites. These are: Great Britain, Spain and Portugal, Italy, Norway and Sweden. It is not clear to which part Austria and Switzerland belong. These satellites can be very loosely connected to the center. For example Scandinavia is only connected using 2 edges with the rest. These two edges are the two highway sides of a bridge in Copenhagen. This is the 2-edge cut with 73% imbalance found by FlowCutter and InertialFlow. Apparently the ferries to and from Scandinavia are missing in the DIMACS Europe graph and Scandinavia contains about 14% of all nodes. A minimum balanced cut consists of separating the center from its satellites. KaHip finds one of these satellite-cuts. FlowCutter with the distance piercing heuristic does not. FlowCutter finds a Rhine-cut through central Europe. It goes mostly along the Rhine, and then goes along the border between Italy and Austria.

At the first glance it seems as if KaHip wins on this instance. However, in nested dissection context satellite-cuts are not necessarily beneficial. Choosing a satellite-cut at the top level only delays the inevitable Rhine-cut by one level in the separator tree. Theory [9] predicts that picking a small balanced cut  $C$  at the top level is good when the cuts in both resulting sides

are significantly smaller than  $C$ . However, the top levels of the Europe graph does not have this structure. A second level Rhine-cut is significantly larger than a top level satellite-cut. Further the union of the satellites are only very loosely connected. This is a huge contrast to the large Rhine-cut needed for the other side. The satellite-cuts are thus highly imbalanced in this sense. This is the reason why KaHip’s finding a smaller top level cut does not contradict FlowCutter producing better contraction orders.

A question that arises is whether the cut found by KaHip is the best cut separating the center from the satellites. To investigate this question we run FlowCutter with handpicked multiple source and target nodes. We pick a source node in the middle of Europe and a target node in each of the 4 satellites. We pick the closest nodes to the coordinates reported in Table 6. FlowCutter does not find the 112-edge cut with 8% imbalance found by KaHip. It does however find a probably superior satellite-cut with 87 edges and 15% imbalance that KaHip misses. This cut is illustrated in Figure 7b. The main difference is to which side Austria belongs. Also the cut through Switzerland and the cut at the France-Spanish border differs slightly.

	Lat	Lon	Place
Source	49.0	8.4	Karlsruhe
	41.0	16.9	Bari
Target	38.7	-9.1	Lisbon
	53.5	-2.8	Liverpool
	59.2	18.0	Stockholm

Table 6: Handpicked source and target nodes.

max $\epsilon$ [%]	Achieved $\epsilon$ [%]				Cut Size				Running Time [s]			
	F20	K	M	I	F20	K	M	I	F20	K	M	I
0	0.000	0.000	0.001	0.000	37	74	40	259	12.1	4.5	0.1	0.2
1	0.277	0.970	0.002	0.088	29	34	39	96	9.9	2.8	0.2	0.3
3	0.277	2.999	0.000	0.748	29	29	51	70	9.9	4.0	0.2	0.3
5	4.263	4.290	0.025	0.897	28	27	40	60	9.6	5.1	0.1	0.3
10	9.073	9.467	0.001	1.413	23	23	47	46	8.1	9.1	0.2	0.3
20	19.995	11.761	16.671	13.984	19	22	376	27	6.8	3.2	0.2	0.3
30	27.606	12.249	23.080	23.125	14	20	521	21	5.2	3.0	0.2	0.4
50	40.630	9.772	42.409	36.365	12	23	14	14	4.5	3.4	0.1	0.4
70	57.602	12.000	41.177	48.771	11	23	1124	12	4.2	3.5	0.2	0.5
90	87.330	12.084	47.362	81.495	8	20	856	9	3.1	3.5	0.2	0.6

Table 7: Results for the DIMACS Colorado graph with 436K nodes and 521K edges. In [5] it was shown that an optimal perfectly balanced cut has 29 edges.

max $\epsilon$ [%]	Achieved $\epsilon$ [%]				Cut Size				Running Time [s]			
	F20	K	M	I	F20	K	M	I	F20	K	M	I
0	0.000	0.000	0.001	0.000	119	1342	245	1579	1902.0	2489.1	12.2	15.7
1	0.594	0.545	0.000	0.388	86	109	216	406	1717.6	274.7	12.1	23.6
3	2.333	2.334	0.001	0.071	76	76	204	257	1584.2	720.8	12.2	31.7
5	3.844	3.845	0.001	0.102	61	61	255	186	1377.5	1262.3	12.4	35.5
10	3.844	3.846	0.000	3.169	61	61	196	81	1377.5	2073.7	12.4	29.7
20	3.844	3.850	0.001	3.866	61	61	138	61	1377.5	249.0	12.2	45.6
30	3.844	3.850	0.001	3.866	61	61	232	61	1377.5	249.1	12.3	64.8
50	3.844	3.850	0.001	3.866	61	61	198	61	1377.5	248.8	12.4	100.7
70	69.575	3.850	41.178	66.537	46	61	64414	61	1056.2	249.6	12.9	158.7
90	89.350	3.850	47.370	70.315	42	61	60071	46	965.2	249.2	12.8	201.1

Table 8: Results for the DIMACS USA graph with 24M nodes and 29M edges.

## C Further Experiments

Tables 7 and 8 contain further Pareto-set experiments. The observed effects essentially follow those already discussed for Table 2.

## D Detailed Running Time Analysis

The lines 1-3 have a running time in  $O(m)$  and are therefore unproblematic. The condition in line 4 can be implemented in  $O(1)$  as following:  $S$  and  $T$  only grow. We can therefore check when adding a node to one of the sets, whether it is contained in the other set. If this is the case we abort the loop. Outside of the true-branch of the if-statement in line 5 also  $S_R$  and  $T_R$  only grow. We can therefore use the same argument for the condition in line 5. Lines 6-8 need  $O(m)$  running time each time they are executed. However, they are only executed when the flow is augmented. This happens  $c$  times. The total running time is thus in  $O(cm)$ . Showing that the running time of the lines 11-16 is amortized sub-linear is the complex part of the analysis. Implementing the growing operations in lines 11 and 16 the naive way needs linear running time and is therefore too slow. The naive approach looks at all internal nodes to determine all outgoing edges. These are needed to determine which are the non-saturated edges. However, either the sets only contain a single node  $x$  or they were generated by growing them and afterwards adding a single additional node  $y$ . In either case it is sufficient to look at the outgoing edges of  $x$  or  $y$  because all other outgoing edges must be saturated, as otherwise they would have been followed in a previous iteration. Outputting the cut in line 12 causes costs linear in the cut size. We account for these when calling the piercing oracle in line 13. However, it is non-trivial that we can list all edges in the cut in linear time. We do this by maintaining two additional edge sets  $C_S$  and  $C_T$ . The source side cut is in  $C_S$  and the target side cut is in  $C_T$ . We only describe how to maintain  $C_S$ . The algorithm for  $C_T$  is analogous. Each time we grow  $S$  and the graph search algorithm encounters a saturated edge  $e$  it adds  $e$  to  $C_S$ . Every cut edge is saturated and therefore the desired cut is a subset of  $C_S$ . As  $S$  never shrinks each edge can only be added at most once and therefore these additions have running time costs within  $O(m)$ . In line 12 it is possible that  $C_S$  contains edges that are saturated but not part of the cut. We filter those edges by iterating over all edges and removing those for which both end points are in  $S$ . As each edge can be removed at most once the removal costs are within  $O(m)$ . The remaining edges are the cut. We account for the running needed to skip the cut edges during the filter step when calling the piercing oracle in line 13. The lines 14-15 have a constant running time. It remains to show that all the calls to the piercing oracle in line 13 in total do not need more than  $O(cm)$  running time. The key observation here is that each time that the oracle is called it names a piercing arc  $e$ . The next time the oracle is called  $e$  is no longer part of the cut and therefore the oracle can no longer return  $e$ . Each edge is therefore only at most in one iteration the piercing arc. The oracle is therefore called at most  $m$  times. Each time it has a running time linear in the cut size. We can bound the cut size of each step by the final cut size  $c$  as the cut sizes only increases. The total running time spent in the piercing oracle is therefore bound by  $O(cm)$ .